

# Calculation of the Potential Energy Surface for Intermolecular Amide Hydrogen Bonds Using Semiempirical and *Ab Initio* Methods

Helgi Adalsteinsson,<sup>1</sup> Andreas H. Maulitz, and Thomas C. Bruice\*

Contribution from the Department of Chemistry, University of California at Santa Barbara, Santa Barbara, California 93106

Received December 20, 1995<sup>⊗</sup>

**Abstract:** The dependence of hydrogen-bond interaction energies between identical amides (two formamides and two *N*-methylacetamides) on the hydrogen bond length ( $r_{O\cdots H}$ ), the two hydrogen bond angles ( $\theta_{COH}$  and  $\theta_{NHO}$ ), and the dihedral between the two amides ( $\Phi_{CNCN}$ ) has been assessed by semiempirical calculations (SAM1 with single point transfers to AM1/SM2.1 aqueous solvation calculations). *Ab initio* calculations (MP2/6-31+G(d,p)//HF/6-31+G(d,p)) at given values of  $\Phi_{CNCN}$  and  $\theta_{COH}$  predict the same change in interaction energies with changes in  $\theta_{NHO}$  as the semiempirical calculations. With formamide, hydrogen-bond interaction energies are independent of the dihedral angle  $\Phi_{CNCN}$  when  $\theta_{COH}$  and  $\theta_{NHO}$  deviate less than 40° from 180°. Most importantly, the increased interaction energies at  $\theta_{COH}$  and  $\theta_{NHO}$  below 140° and above 220° are found to be associated with steric interference between the carbonyl oxygen of the hydrogen-bond acceptor and the amide nitrogen of the hydrogen-bond donor. Comparing formamide and *N*-methylacetamide, the angle requirements ( $\theta_{COH}$ ,  $\theta_{NHO}$ , and  $\Phi_{CNCN}$ ) of favorable hydrogen-bond interaction energies are much more stringent for the latter due to the steric effects of the methyl substituents. In summary, by both semiempirical SAM1 and *ab initio* MP2/6-31+G(d,p)//HF/6-31+G(d,p) calculations, the strength of amide hydrogen bonding in the absence of steric hindrance is essentially independent of the angles defining the hydrogen bond.

## Introduction

Hydrogen bonding is undoubtedly one of the chemical worlds most interesting phenomena due to the crucial role it plays in the structure and interactions of biomolecules. Experimental data for hydrogen bonding in proteins has been organized and summarized carefully by Baker and Hubbard,<sup>2</sup> but those results do not show the relative stability of different hydrogen-bonding conformations. They do, on the other hand, form a library to which the results from other studies can be compared. A study by Murray-Rust and Glusker<sup>3</sup> examined the directionality of hydrogen bonding to oxygen atoms of ether, ketone, epoxide, enone, and ester groups using the Cambridge Structural Database System.<sup>4</sup> Various studies have been performed with simple amide model systems using both experimental<sup>4–8</sup> and computational<sup>9–15</sup> approaches. Computations of hydrogen bond

strengths between the carbonyl oxygen and the amide proton of two identical amides have been carried out with formamide,<sup>9–13</sup> *N*-methylacetamide,<sup>9,10,12,14–17</sup> simple peptides,<sup>11,12</sup> and assorted other systems.<sup>10,15,17</sup> These calculations have primarily been performed using *ab initio* computational methods. Most of the studies are limited to a coplanar arrangement and only a few have examined the effect of different orientations between the two amides. Additionally, most of the studies do not examine the effect of varying both hydrogen-bonding angles, but only examine the effect of varying the N–H $\cdots$ O angle.

This study examines the dependence of hydrogen-bond strength of intermolecular hydrogen bonds on the hydrogen-bonding distance ( $r_{O\cdots H}$ ), the two hydrogen-bond angles ( $\theta_{NHO}$  and  $\theta_{COH}$ ), and the intermolecular dihedral angle ( $\Phi_{CNCN}$ ) (Chart 1). To do so requires examination of the potential energy surface of intermolecular amide hydrogen bonding in much greater detail than is feasible using reliable *ab initio* methods. The potential energy surfaces have been determined by semiempirical SAM1<sup>18</sup> calculations, which have been shown to be more reliable than other semiempirical methods in evaluating hydrogen-bond energies,<sup>18c</sup> and select results verified by *ab initio* calculations at the MP2/6-31+G(d,p)//HF/6-31+G(d,p) level of theory. In order to model hydrogen bonding in aqueous solution, the aqueous potential energies were calculated using the AM1/SM2.1 solvation model.<sup>20,21</sup>

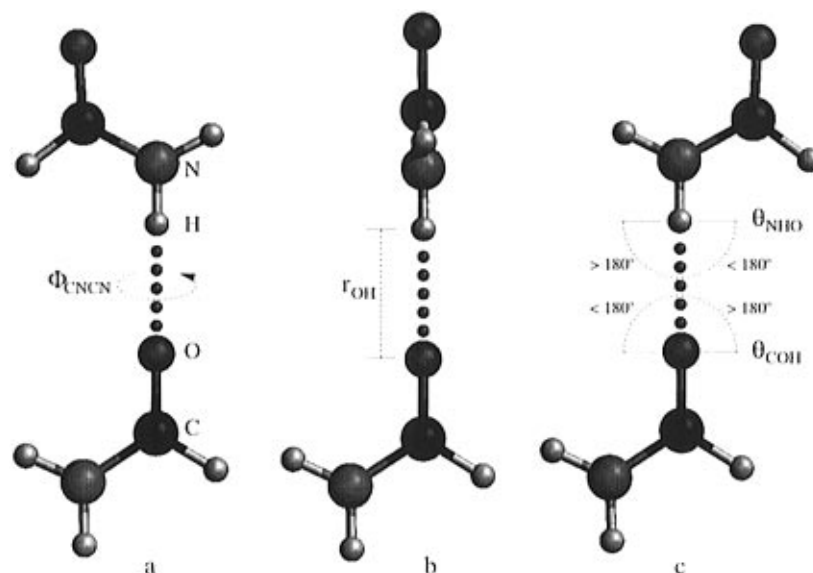
<sup>⊗</sup> Abstract published in *Advance ACS Abstracts*, August 1, 1996.

- (1) In partial satisfaction of Ph.D. requirements.
- (2) Baker, E. N.; Hubbard, R. E. *Prog. Biophys. Mol. Biol.* **1984**, *44*, 97.
- (3) Murray-Rust, P.; Glusker, J. P. *J. Am. Chem. Soc.* **1984**, *106*, 1018.
- (4) Dado, G. P.; Desper, J. M.; Gellman, S. H. *J. Am. Chem. Soc.* **1990**, *112*, 8630.
- (5) Gellman, S. H.; Dado, G. P.; Liang, G.-B.; Adams, B. R. *J. Am. Chem. Soc.* **1991**, *113*, 1164.
- (6) Eberhardt, E. S.; Raines, R. T. *J. Am. Chem. Soc.* **1994**, *116*, 2149.
- (7) Gardner, R. R.; Gellman, S. H. *J. Am. Chem. Soc.* **1995**, *117*, 10411.
- (8) Taylor, R.; Kennard, O. *Acc. Chem. Res.* **1984**, *17*, 320.
- (9) Johansson, A.; Kollman, P.; Rothenberg, S.; McKelvey, J. *J. Am. Chem. Soc.* **1974**, *96*, 3794.
- (10) Kolaskar, A. S.; Lakshminarayanan, A. V.; Sarathy, K. P.; Saissekharan, V. *Biopolymers* **1975**, *14*, 1081.
- (11) Peters, D.; Peters, J. *J. Mol. Struct.* **1980**, *68*, 255.
- (12) Sapse, A. M.; Fugler, L. M.; Cowburn, D. *Int. J. Quantum Chem.* **1986**, *29*, 1241.
- (13) Novoa, J. J.; Whangbo, M.-H. *J. Am. Chem. Soc.* **1991**, *113*, 9017.
- (14) Ramachandran, G. N.; Lakshminarayanan, A. V.; Kolaskar, A. S. *Biochim. Biophys. Acta* **1973**, *303*, 8.
- (15) Guo, H.; Karplus, M. *J. Phys. Chem.* **1992**, *96*, 7273.

(16) Renugopalakrishnan, V.; Rein, R. *Biochim. Biophys. Acta* **1976**, *434*, 164.

- (17) Cheam, T. C.; Krimm, S. *J. Mol. Struct.* **1986**, *146*, 175.
- (18) (a) Dewar, M. J. S.; Jie, C.; Yu, G. *Tetrahedron* **1993**, *23*, 5003.
- (b) Holder, A. J.; Dennington, R. D.; Jie, C. *Tetrahedron* **1994**, *50*, 627.
- (c) Holder, A. J.; Evleth, E. M. In *Modeling the Hydrogen Bond*; Smith, D. A., Ed.; American Chemical Society: Washington, DC, 1994; pp 113.
- (19) Ampac 5.0, 1994 Semichem, 7128 Summit, Shawnee, KS 66216.
- (20) Dewar, M. J. S.; Zoebisch, E. G.; Healy, E. F.; Stewart, J. J. P. *J. Am. Chem. Soc.* **1985**, *107*, 3902.
- (21) Cramer, C. J.; Truhlar, D. G. *J. CAMD* **1992**, *6*, 629.

Chart 1



### Experimental Section

The procedures described below apply to both formamide dimer and *N*-methylacetamide dimer calculations. Semiempirical gas phase geometry minimizations were performed using the semiempirical SAM1<sup>18</sup> method in the program Ampac 5.0.<sup>19</sup> Interaction energies (IE) were determined by subtracting twice the calculated heat of formation for a geometry-optimized amide monomer from the heat of formation calculated for the dimers. Hydrogen bonding was only considered for the hydrogen *trans* to the carbonyl oxygen. *N*-Methylacetamide was arranged such that the amide methyl group was *cis* to the carbonyl oxygen. After constrained gas phase geometry optimizations had been completed, single-point aqueous solvation energies were calculated for the resulting geometries using the semiempirical AM1<sup>20</sup> method along with the SM2.1<sup>21</sup> aqueous solvation model, yielding aqueous interaction energies. Constrained *ab initio* HF/6-31+G(d,p) geometry optimizations were performed for select geometries from the potential energy surface using Spartan 4.0.4.<sup>22</sup> MP2/6-31+G(d,p) single point energies were calculated for the resulting geometries using Gaussian 94.<sup>23</sup>

The degrees of freedom examined for the potential energy surface are shown in Chart 1. For each of the three dihedral angles evaluated ( $\Phi_{\text{CNCN}} = 0^\circ, 90^\circ, \text{ and } 180^\circ$  respectively), seven  $\text{C}=\text{O}\cdots\text{H}$  hydrogen-bonding angles ( $\theta_{\text{COH}}$ ) ranging between  $120^\circ$  and  $240^\circ$  in  $20^\circ$  intervals were examined. Within each fixed  $\theta_{\text{COH}}$ , 45  $\text{O}\cdots\text{H}$  hydrogen-bonding distances ( $r_{\text{O}\cdots\text{H}}$ ) were investigated from  $1.75 \text{ \AA}$  to  $3.5 \text{ \AA}$ . At each of these fixed hydrogen-bonding distances we carried out 60 calculations of the  $\text{N}-\text{H}\cdots\text{O}$  hydrogen-bonding angle ( $\theta_{\text{NHO}}$ ) incremented from  $120^\circ$  to  $240^\circ$ . The semiempirically calculated five-dimensional potential energy surfaces thus obtained for formamide and *N*-methylacetamide consist of 56 700 points each. Several three-dimensional potential energy surfaces were plotted for each of the systems to visualize the interaction energies of the corresponding geometries as a function of the variables being incremented. The surfaces were used to determine the location and shape of the hydrogen-bonding energy minimum, and select cross sections of each surface were used to examine the effect of each variable on the hydrogen-bond interaction energies.

### Results

**Formamide interaction energy dependence on  $\theta_{\text{NHO}}$**  was found to be in the range of  $0.2\text{--}0.3 \text{ kcal/mol}$  when  $140^\circ < \theta_{\text{NHO}} < 220^\circ$  and  $140^\circ < \theta_{\text{COH}} < 220^\circ$ . A representative surface is shown in Figure 1, displaying semiempirical gas phase IE as a function of  $r_{\text{O}\cdots\text{H}}$  and  $\theta_{\text{NHO}}$  at  $\theta_{\text{COH}} = 160^\circ$  and  $\Phi_{\text{CNCN}} = 180^\circ$ . The depression in the surface (colored red) corresponds

to the most favorable IE. A cross section of the surface is shown in Figure 2, along with comparative studies using AM1/SM2.1 aqueous solvation calculations and *ab initio* MP2/6-31+G(d,p)/HF/6-31+G(d,p) calculations. From these studies it is apparent that the three different methods agree on the variation in interaction energy for the change in  $\theta_{\text{NHO}}$  specified above, although the absolute calculated interaction energies are different. The result is the same for all dihedral angles examined (see below). Semiempirical gas phase IE surfaces calculated for formamide and *N*-methylacetamide with  $\Phi_{\text{CNCN}}$  fixed at  $180^\circ$  and  $\theta_{\text{COH}}$  fixed at  $160^\circ$  are shown in Figures 1 and 3, respectively. Forty-two such potential energy surface cross sections were generated for visualization.

**The dependence of the formamide interaction energy on  $\theta_{\text{COH}}$**  was found to be less than the dependence upon  $\theta_{\text{NHO}}$ . An examination of the potential energy surface where the angles associated with the  $\text{CO}\cdots\text{H}$  geometry were varied ( $\theta_{\text{COH}}$  and  $\Phi_{\text{NCOH}}$ , Chart 2) shows  $\theta_{\text{COH}} = 140^\circ$  to be favored by a mere  $0.1 \text{ kcal/mol}$  over  $\theta_{\text{COH}} = 180^\circ$  (sections I and II in Figure 5). In Figure 5, the effect of varying  $\theta_{\text{COH}}$  at  $r_{\text{O}\cdots\text{H}} = 1.9 \text{ \AA}$  and  $\Phi_{\text{CNCN}} = 180^\circ$  on the calculated semiempirical gas phase and aqueous interaction energies is shown. This cross section displays a  $0.1 \text{ kcal/mol}$  preference for hydrogen-bond angles corresponding to the positions of the lone pairs of the carbonyl oxygen.

**Dependence of the formamide interaction energy on  $r_{\text{O}\cdots\text{H}}$**  was examined in both gas phase and aqueous solvation semiempirical calculations. The gas phase calculations predict on optimal hydrogen-bonding distance of  $1.94 \text{ \AA}$  with a large increase in IE for long hydrogen bonds. The aqueous solvation calculations predict an optimal hydrogen bonding distance of  $2.20 \text{ \AA}$  and a much smaller change in IE for long hydrogen bonds.

**Dependence of the formamide interaction energy on  $\Phi_{\text{CNCN}}$**  was found to be insignificant ( $\sim 0.02 \text{ kcal/mol}$ ) in the absence of steric limitations. The steric limitations due to van

(22) Spartan version 4.0.4, Wavefunction, Inc., 18401 Von Karman Ave. #370, Irvine, CA 92715.

(23) Frisch, M. J.; Trucks, G. W.; Schlegel, H. B.; Gill, P. M. W.; Johnson, B. G.; Robb, M. A.; Cheeseman, J. R.; Keith, T. A.; Petersson, G. A.; Montgomery, J. A.; Raghavahari, K.; Al-Laham, M. A.; Zakrzewski, V. G.; Ortiz, J. V.; Foresman, J. B.; Cioslowski, J.; Stefanov, B. B.; Nanayakkara, A.; Challacombe, M.; Peng, C. Y.; Ayala, P. Y.; Chen, W.; Wong, M. W.; Andres, J. L.; Replogle, E. S.; Gomperts, R.; Martin, R. L.; Fox, D. J.; Binkley, J. S.; Defrees, D. J.; Baker, J.; Stewart, J. P.; Head-Gordon, M.; Gonzales, C.; Pople, J. A. *Gaussian 94 (Revision A.1)*; Gaussian, Inc., Pittsburgh, PA, 1995.

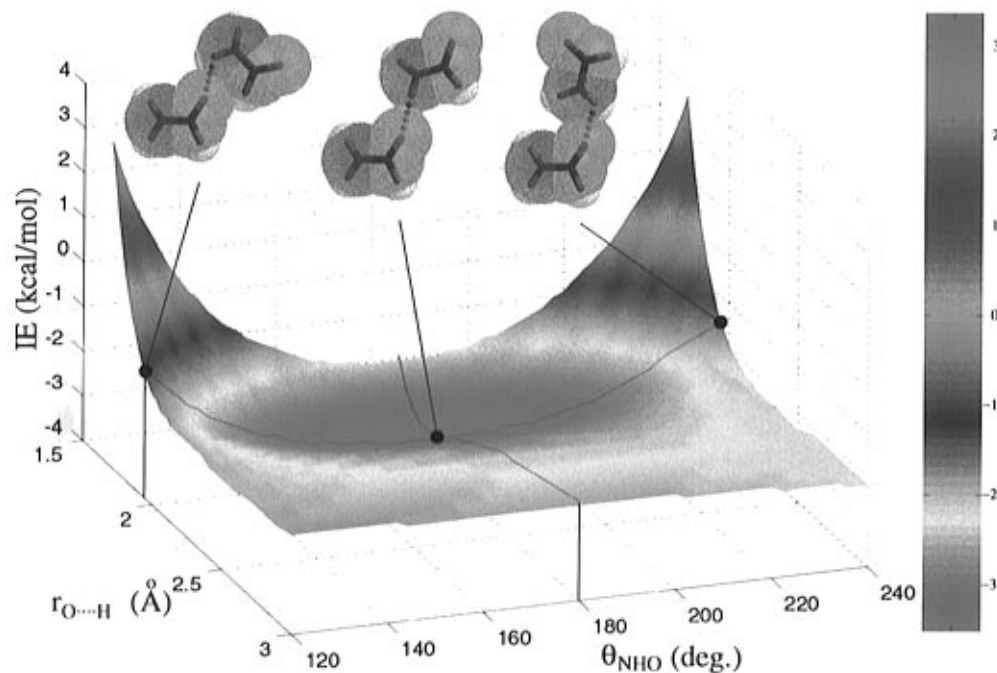


**Figure 1.** A sample cross section of the potential energy surface of intermolecular formamide hydrogen bonding showing the dependence of semiempirical gas phase interaction energies upon  $r_{\text{OH}}$  and  $\theta_{\text{NHO}}$  ( $\Phi_{\text{CNCN}} = 180^\circ$ ,  $\theta_{\text{COH}} = 160^\circ$ ). The structures show the optimum geometry (center) and the steric hindrance accompanying van der Waals overlap between carbonyl oxygen acceptor and amide nitrogen donor. The  $\theta_{\text{NHO}}$  cross section in Figure 2 is shown as a line through the surface at  $r_{\text{OH}} = 2.0 \text{ \AA}$ .

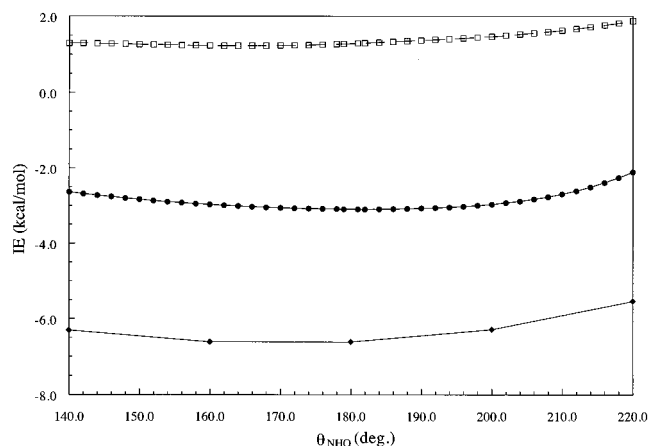


**Figure 2.** Interaction energies for formamide hydrogen bonding plotted vs bond angle  $\theta_{\text{NHO}}$ . Computed via SAM1 (●), AM1/SM2.1 (□), and MP2/6-31+G(d,p)//HF/6-31+G(d,p) (◆) ( $r_{\text{OH}} = 2.1 \text{ \AA}$ ,  $\theta_{\text{COH}} = 160^\circ$ ,  $\Phi_{\text{CNCN}} = 180^\circ$ ). Inspection shows that though the interaction energies vary greatly, dependent upon the mode of calculation, the change in interaction energies with change in  $\theta_{\text{NHO}}$  are quite comparable.

der Waals overlap between the hydrogen bond-donor nitrogen and the hydrogen-bond-acceptor carbonyl oxygen were not relieved by change in  $\Phi_{\text{CNCN}}$ .

**Steric limitations on the interaction energies of formamide** were found to be the only forces at constant  $r_{\text{O}\cdots\text{H}}$  that limit feasible hydrogen bonding. When the distance between the hydrogen-bond-donor nitrogen and the hydrogen-bond-acceptor oxygen fell below  $2.5 \text{ \AA}$ , which is well within van der Waals contact for nitrogen and oxygen, the interaction energies rose sharply as expected. The angle flexibility of the hydrogen-bonded dimer, therefore, decreases rapidly at short hydrogen-bonding distances, thus, favoring linear hydrogen-bonding geometry (Figure 1).

**N-Methylacetamide** displays similar features in the calculated potential energy surface as formamide. Most significantly, the steric limitations on favorable conformations for periplanar

dimer arrangement ( $\Phi_{\text{CNCN}} = 0^\circ$  or  $180^\circ$ ) are much more pronounced than for formamide. This can clearly be attributed to the greater size of the methyl as compared to the hydrogen substituents. The potential energy surface therefore displays a significant energy stabilization upon twisting the two amide units out of their common plane. In the absence of steric limitations, interaction energies are independent of the degrees of freedom defining the hydrogen bond. The *N*-methylacetamide calculations also show a more pronounced tendency to relieve unfavorable steric interactions by varying the other degrees of freedom associated with the hydrogen bond, such as the hydrogen-bonding angles and distance, than the formamide calculations do.

## Discussion

**The formamide potential energy surface** predicts  $0.2\text{--}0.3$  kcal/mol variations in interaction energy when either  $\theta_{\text{NHO}}$  or  $\theta_{\text{COH}}$  deviate less than  $40^\circ$  from  $180^\circ$  and the other hydrogen-bonding angle is equal to  $180^\circ$ . Earlier semiempirical AM1 calculations of hydrogen bonding of two formamides showed no change in interaction energy upon changing the hydrogen-bonding angles; however, HF/6-31G\*\* calculations showed changes exceeding  $1 \text{ kcal/mol}$ .<sup>13</sup> The dependence of interaction energies upon hydrogen-bond angles predicted by our semiempirical SAM1 calculations correlate very well with our predictions from *ab initio* MP2/6-31+G(d,p)//HF/6-31+G(d,p) calculations (Figure 2), but the SAM1 interaction energies are almost  $4 \text{ kcal/mol}$  higher than those found by *ab initio* MP2/6-31+G(d,p)//HF/6-31+G(d,p) calculations. It has been observed that a procedure which gives poor estimates of free energies of individual molecules may reproduce the difference in free energy between reactants and products in a reaction correctly.<sup>24</sup> The excellent agreement between the changes in interaction energies using semiempirical SAM1 and *ab initio* MP2/6-31+G(d,p)//HF/6-31+G(d,p) calculations gives a good indication that this is the case here. The calculated semiem-

(24) Dewar, M. J. S.; Jie, C.; Yu, J. *Tetrahedron* **1993**, *23*, 5003.

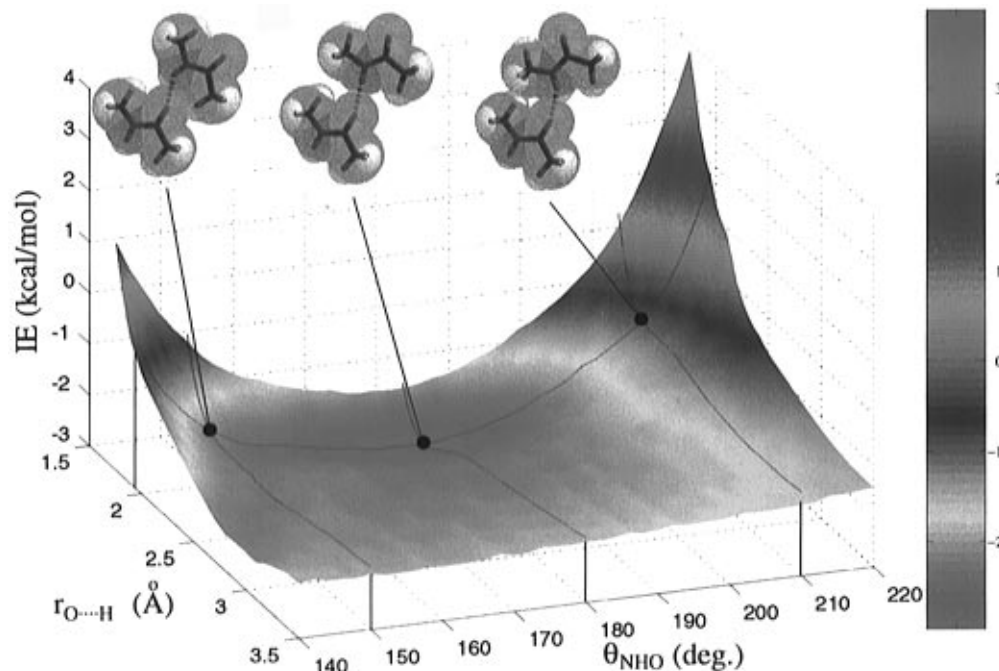
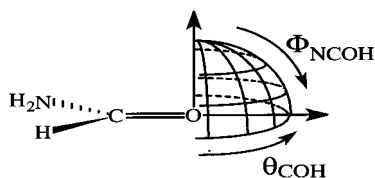


**Figure 3.** A sample cross section of the potential energy surface of intermolecular *N*-methylacetamide hydrogen bonding showing the dependence of semiempirical gas phase interaction energies upon  $r_{\text{OH}}$  and  $\theta_{\text{NHO}}$  for intermolecular *N*-methylacetamides hydrogen bonding ( $\Phi_{\text{CNCN}} = 180^\circ$ ,  $\theta_{\text{COH}} = 160^\circ$ ). The structures show the optimum geometry (center) and the steric hindrance accompanying van der Waals overlap between carbonyl oxygen and acetamide methyl group (left) and two amide methyl groups (right). The  $\theta_{\text{NHO}}$  cross section in Figure 4 is shown as a line at  $r_{\text{OH}} = 2.0 \text{ \AA}$ .

#### Chart 2



pirical aqueous enthalpy angle dependency determined by AM1/SM2.1 aqueous solvation calculations also correlates well with the results from the *ab initio* gas phase calculations mentioned above (Figure 2). The interaction energies calculated in the aqueous solvation model are about 1 kcal/mol; i.e., the calculations predict that the hydrogen-bonded formamide dimer is less stable in water than the non-hydrogen-bonded monomers. This corresponds well with published *ab initio* calculations which show that an amide–amide hydrogen bond to an amide proton *trans* to the carbonyl oxygen is about as strong as the corresponding amide–water hydrogen bond.<sup>25</sup> The change in interaction energies due to modest changes in hydrogen bond angles ( $\theta_{\text{NHO}}$  or  $\theta_{\text{COH}}$  varied less than  $40^\circ$  from linear) are usually fairly small. For example, our calculated increase in interaction energy when narrowing  $\theta_{\text{NHO}}$  from  $180^\circ$  to  $140^\circ$  ( $\theta_{\text{COH}}$  at  $160^\circ$  and  $\Phi_{\text{CNCN}}$  at  $180^\circ$ ) is 0.2 kcal/mol (Figure 2). As mentioned above, an examination of the potential energy surface where the angles associated with the  $\text{CO}\cdots\text{H}$  geometry were varied ( $\theta_{\text{COH}}$  and  $\Phi_{\text{NCOH}}$ , Chart 2) shows  $\theta_{\text{COH}} = 140^\circ$  to be favored by a mere 0.1 kcal/mol over  $\theta_{\text{COH}} = 180^\circ$ . This is in agreement with the finding that “there is a statistically significant tendency for hydrogen bonds to occur within about  $13^\circ$  of the lone-pair plane and  $10^\circ$  of the idealized  $\text{sp}^2$  lone-pair direction”<sup>8</sup> in the crystal structures of a number of  $\text{N}-\text{H}\cdots\text{O}=\text{C}$  hydrogen bonded compounds. A study by Murray-Rust and Glusker examined hydrogen bonding in several

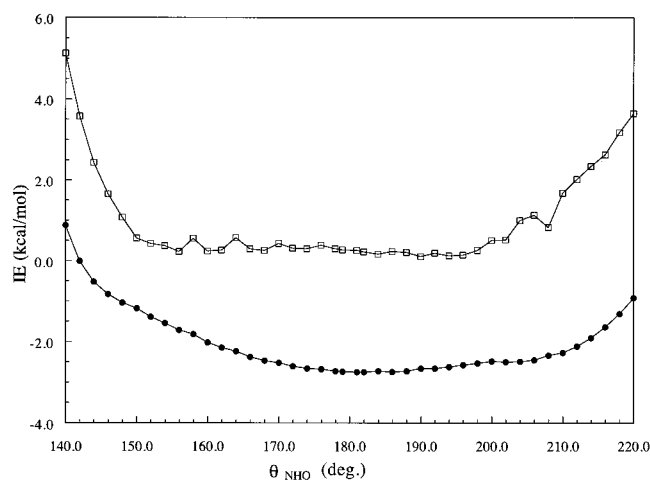


**Figure 4.** Interaction energies for *N*-methylacetamide hydrogen bonding plotted vs bond angle  $\theta_{\text{NHO}}$  ( $r_{\text{OH}} = 2.1 \text{ \AA}$ ,  $\theta_{\text{COH}} = 160^\circ$ ,  $\Phi_{\text{CNCN}} = 180^\circ$ ). Computed via SAMI (●) and AM1/SM2.1 (□). Comparing the results to formamide, the sensitivity to  $\theta_{\text{NHO}}$  is greatly increased due to the acetyl and amide methyl groups.

hundred crystal structures of ethers, ketones, enones, epoxides, and esters.<sup>3</sup> This study showed a wide distribution of  $\theta_{\text{COH}}$  angles, with a marked tendency for hydrogen bonds to occur at the lone-pair directions of carbonyl oxygens. We find that when the distance between the hydrogen-bond-donor nitrogen and the hydrogen-bond-acceptor oxygen is below  $2.5 \text{ \AA}$ , well within van der Waals contact for the two atoms, the interaction energies rise sharply. The flexibility of the hydrogen-bonded dimer, therefore, decreases rapidly at short hydrogen-bonding distances, favoring linear hydrogen-bonding geometry. This corresponds very well with the experimental observation that  $\text{N}-\text{H}\cdots\text{O}$  hydrogen bonds show an increased preference for linearity at short  $r_{\text{O}\cdots\text{H}}$  distances.<sup>8</sup> It is well-known that interaction energies rise sharply upon bringing two molecules into van der Waals contact. On doing so, the hydrogen-donor and -acceptor atoms

(25) Dixon, D. A.; Dobbs, K. D.; Valentini, J. J. *J. Phys. Chem.* **1994**, *98*, 13435.

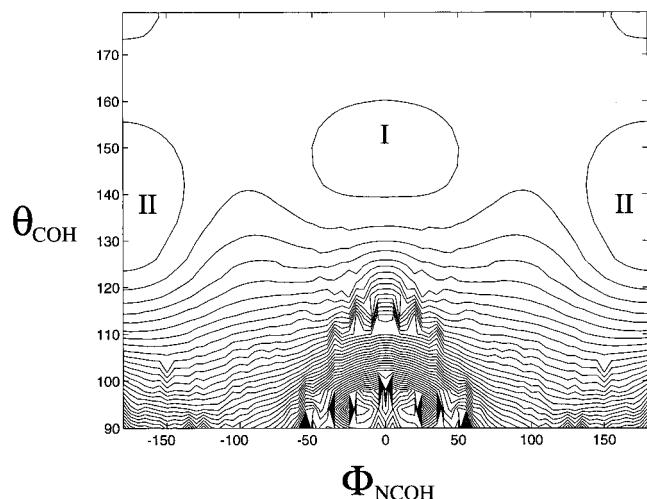


**Figure 5.** A contour plot of the potential energy surface generated by varying the angles  $\Phi_{\text{NCOH}}$  and  $\theta_{\text{COH}}$  associated with the hydrogen-bond geometry around the hydrogen-bond-acceptor carbonyl oxygen (Chart 2). Labels I and II mark areas of minimum energy, corresponding to the two lone pair positions on the carbonyl oxygen. Contour line spacing is 0.1 kcal/mol.

approach such that the dependence of interaction energies upon  $\theta_{\text{NHO}}$  or  $\theta_{\text{COH}}$  increases.

The *N*-methylacetamide potential energy surface displays a well-defined optimal region for intermolecular hydrogen bonds (Figure 3). Cross sections of the potential energy surface predict a significant increase in interaction energy from steric influences upon changing either  $\theta_{\text{COH}}$  or  $\theta_{\text{NHO}}$  from their preferred values (Figure 4). Steric hindrance to hydrogen bonding is much greater than for formamide due to the size of the acetamide and amide methyl groups. Systems having  $\theta_{\text{COH}}$  or  $\theta_{\text{NHO}}$  narrower than  $140^\circ$  were not examined, since the calculated interaction energy rose sharply outside those limits. Steric effects are minimized by rotation about  $\Phi_{\text{CNCN}}$  resulting in greater stability at  $\Phi_{\text{CNCN}} \approx 90^\circ$ , a conformation similar to that shown in Chart 1b, in which the acetamides are not coplanar. This is consistent with the result that the angular energy dependency is less when the planes of the two amides are perpendicular than when they are parallel. This difference is much more pronounced for *N*-methylacetamide than for formamide. When both amides are in the same plane (Chart 1

structures **a** and **c**), bending of hydrogen bond angles  $\theta_{\text{COH}}$  and  $\theta_{\text{NHO}}$  from  $180^\circ$  brings the methyl groups into contact, causing the calculated interaction energy to rise. Thus, the calculated penalty for hydrogen-bonding angles  $\theta_{\text{COH}}$  or  $\theta_{\text{NHO}}$  deviating more than  $20^\circ$  from  $180^\circ$  is much lower when the planes of the amides are perpendicular than when they are parallel. The calculations also predict that an unfavorable hydrogen bonding angle ( $\theta_{\text{COH}}$  or  $\theta_{\text{NHO}}$ ) can be compensated for by bending the other hydrogen bonding angle in the opposite direction. That is what would be expected from the potential energy surface found for intermolecular formamide hydrogen bonding (Figure 1). On the basis of these observations, one would predict steric effects to be the main determining factor in controlling hydrogen-bonding geometry in proteins, with hydrogen-bond length being the only term that is sensitive to variations.

## Conclusion

The geometry of hydrogen bonding between amides can be described in terms of hydrogen bond length ( $r_{\text{O}\cdots\text{H}}$ ), the two hydrogen bond angles ( $\theta_{\text{COH}}$  and  $\theta_{\text{NHO}}$ ), and the dihedral between the two amides ( $\Phi_{\text{CNCN}}$ , Chart 1). At an optimum  $r_{\text{O}\cdots\text{H}}$  distance ( $2.1 \text{ \AA}$ ), and with the very minimum of steric overlap (formamide,  $\Phi_{\text{CNCN}} = 90^\circ$ ), there is little or no interaction energy change in hydrogen bonding between two formamides when  $140^\circ < \theta < 220^\circ$  for both  $\theta_{\text{COH}}$  and  $\theta_{\text{NHO}}$ . Outside this range of parameters, the interaction energy increases precipitously. This is not due to electrostatic factors involving the hydrogen bond, but to approach of the van der Waals surfaces of the amide nitrogen of the H-bond donor to the carbonyl oxygen of the H-bond acceptor. The constant interaction energy surface at a given  $r_{\text{O}\cdots\text{H}}$  is much decreased for hydrogen bonding between two *N*-methylacetamides when compared to that of intermolecular formamide hydrogen bonding. The interaction energies calculated for *N*-methylacetamide are much more dependent on the torsion angle between the amides due to the steric hindrance of the larger terminal substituents. To conclude, there is essentially no dependence of the strength of hydrogen bonding between amides on the angles defining the hydrogen bond that is not explained by steric hindrance.

**Acknowledgment.** This work was supported by a grant from the National Institutes of Health (DK09171).

JA954267N